Numerical Analysis of Soil Liquefaction Induced Failure of Earth Dams

Babak Ebrahimian [1,2], Ali Noorzad [1]

1- Faculty of Civil, Water and Environmental Engineering, Abbaspour School of Engineering, Shahid Beheshti University (SBU), Tehran, Iran

2- The Highest Prestigious Scientific and Professional National Foundation, Iran 's National Elites Foundation (INEF), Tehran, Iran

Emails: ebrahimian.babak@gmail.com; b_ebrahimian@sbu.ac.ir

Abstract

This study presents numerical modeling of the dynamic behavior of an earth dam rested on a liquefiable foundation. Numerical simulations are carried out using effective stress-based, fully coupled nonlinear dynamic analysis approach. The Finn-Byrne model with extended Masing rules is employed to model pore pressure generation in the liquefied soils. In this regard, Masing rules are implemented into the constitutive relations to precisely explain the nonlinear response of soil under general cyclic loading. As a result, the soil shear stiffness and hysteretic damping can change with loading history. Pore pressure is accumulated as a function of the cyclic shear strain amplitude. The procedure of calibrating the constructed numerical model with well-documented centrifuge test data is addressed. Acceptable agreements are shown between the results obtained from the current investigation and those of experimental observations available in the literature. Afterwards, the dynamic response of an earth dam founded on a liquefiable sandy soil foundation is evaluated and discussed. Special emphasis is given to the computed excess pore water pressures, deformations and accelerations during dynamic loading. It is shown that the numerical model can predict the essential aspects of liquefaction phenomenon occurred in the earth dam-foundation system during dynamic loading.

Keywords: Numerical simulation, nonlinear dynamic response, liquefaction, earth dam.

1. INTRODUCTION

Soil structures such as embankments and earth dams have been frequently damaged during past major earthquakes in seismically active regions of the world due to the liquefaction of dam materials and/or foundation soils. Many liquefaction induced dam failures or near-failures have been reported during various previous earthquakes [1]. In most cases, large deformations have been occurred due to the liquefaction of the supporting loose cohesionless foundation soil [2]. Experimental studies including shaking table tests [3-4] and centrifuge tests [5-6] and numerical investigations [7-8] related to the liquefaction assessment in embankments and earth dams have been conducted. According to these studies, a complete representation of the failure mechanism usually requires using comprehensive constitutive models accompanied by numerical techniques to account for the effect of generation and dissipation of pore pressure within the dam body and foundation soil and its impact on the variation of shear strength which, in turn, will lead to permanent deformations.

In the current study, the dynamic behavior of an earth dam rested on a liquefiable foundation is numerically simulated by an effective stress-based, fully coupled nonlinear analysis approach. In the following, the numerical modeling procedure is briefly described and then, some aspects related to calibration of the numerical model by using the centrifuge test data are discussed. After verification, a reference model is constructed to represent the basic of dynamic behavior of earth dam founded on a liquefiable soil. A comparative study is performed to identify the effects of liquefiable soils location (in dam, in foundation or in both of them) on the permanent deformations of earth dam, accelerations, pore pressure, liquefaction potential and failure modes of earth dam-foundation system.

2. REVIEW OF NUMERICAL MODELING

In this research, a two-dimensional (2D) reference model is developed to simulate the dynamic behavior of an earth dam founded on liquefiable soil. Nonlinear time history dynamic analysis is conducted using computer program FLAC 2D (Fast Lagrangian Analysis of Continua) [9]. This program is based on a continuum finite difference discretization using the Langrangian approach. For dynamic analysis, it uses an

explicit finite difference scheme to solve the full equation of motion using lumped grid point masses derived from the real density surrounding zone.

Finn and Byrne model is modified and used to carry out coupled effective stress dynamic calculations [10]. The model takes into account the effects of dynamically induced pore water pressures to investigate the degree and extend of liquefaction. First, a static analysis considering the effect of gravity loading is conducted to simulate the stress conditions before the dynamic loading. Once, the initial stress state is established in the model, the reservoir is placed behind the dam. It is noted that the dam and foundation are modeled in several stages corresponding to the stage construction procedure of earth dams. Afterwards, the soil model is changed to a pore pressure generation constitutive model; the effective stress fully coupled dynamic analysis is recalled and started. During the dynamic analysis, the excess pore water pressures are allowed to generate and also the dissipation of these pore pressures is simulated. The selected reference model is a simplified representation of typical earth dam geometry with a symmetric zone section. The numerical grid used in the current study is illustrated in Figure 1.

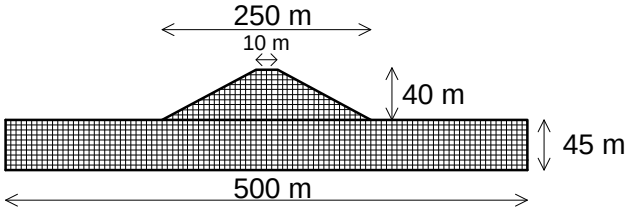

Figure 1. Numerical grid of the dam-foundation system

In static analysis, Mohr-Coulomb constitutive relations are used to model the behavior of sandy soil. The linear behavior is defined by the elastic shear and drained bulk modulus. The shear modulus of sandy soil is calculated with the formula given by Seed and Idriss [11]:

$$G_{\max} = 1000 k_{2\max} \left(\sigma'_m\right)^{0.5} \tag{1}$$

where, G_{max} is the maximum (small strain) shear modulus in pounds per square foot, *psf* (it is later converted to *kPa* to be consistent with the metric units being used), K_{2max} is the shear modulus number (Seed and Idriss [15]), and σ'_m is the mean effective confining stress in *psf*. The Poisson's ratio for sandy soil is taken as 0.3.

For pore water generation during dynamic analysis, the updated model proposed by Byrne [10] is incorporated to account the development of pore water pressure build-up as an effect of volumetric strain induced by the cyclic shear strain using the following formulation:

$$\Delta\varepsilon_v = C_1 \exp\left(C_2 \varepsilon_v / \gamma\right) \tag{2}$$

where, $\Delta\varepsilon_v$ is the increment in volumetric strain that occurs over the current cycle, ε_v is the accumulated volumetric strain for previous cycles, γ is the shear strain amplitude for the current cycle, and C_1 and C_2 are constants dependent on the volumetric strain behavior of the sand. According to Byrne [10], the constant C_1 in Equation (2) controls the amount of volumetric strain increment and C_2 controls the shape of the volumetric strain curve. These constants are estimated using:

$$C_1 = 7600\left(Dr\right)^{-2.5} \tag{3}$$

$$C_2 = 0.4 / C_1 \tag{4}$$

where, *Dr* is the relative density of the soil in percent.

To provide a constitutive model that can better fit the curves of shear modulus degradation and damping ratio increase derived from the experimental tests data, two different modifications are implemented into the FLAC soil model as a part of this research to more precisely assess the potential for predicting liquefaction process and associated deformations. To represent the nonlinear stress-strain behavior of soil more accurately that follows the actual stress-strain path during cyclic loading, the masing rules are implemented into FLAC which works with Byrne model by a FISH subroutine as a first modification. Since, there is a need to accept directly the same degradation curves derived from the test data in fully nonlinear method to model the correct physics, so, the second modification is related to incorporate cyclic data into a hysteretic damping model in FLAC. Modulus degradation curves imply a nonlinear stress-strain curve. An incremental constitutive relation can be derived from the degradation curve, described by $\tau/\gamma = M_s$, where τ is the normalized shear stress, γ is the shear strain and M_s is the normalized secant modulus. The normalized tangent modulus, M_t, is descried as

$$M_t = {d\tau}/{d\gamma} = M_S + \gamma.{dM_S}/{d\gamma} \quad (5)$$

The incremental shear modulus in a nonlinear simulation is then given by GM_t, where G is the small-strain shear modulus of the material. Shear modulus and damping of soils are strain dependent. Shear modulus decreases with increasing shear strain and damping increases with increasing strain. In this study, the shear modulus reduction and Damping ratio increase curves for sandy soils propose by Seed and Idriss are adopted [11]. Geotechnical properties used in the analyses are presented in Table 1 for foundation soil and earth dam materials.

Table 1- Geotechnical soil properties

	γ_d (kN/m^3)	G (MPa)	K (MPa)	Friction (degree)	C_1	C_2
Dam	1520	40	87	30	0.185	2.15
Foundation	1600	60	195	35	0.43	0.93

After static equilibrium is achieved (end of static construction stage), the full width of the foundation is subjected to the variable-amplitude harmonic ground motion record illustrated in Figure 2. The mathematical expression for input acceleration is given by:

$$\ddot{U}(t) = 0.6 \times \sqrt{\beta e^{-\alpha t} t^{\eta}} \sin(2\pi f t) \quad (6)$$

where, α=3.3, β=1.3 and η=10 are constant coefficients, f is the base acceleration frequency and, t is the time.

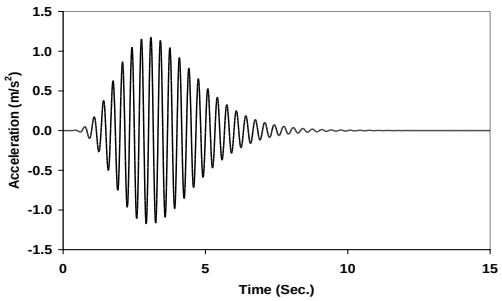

Figure 2. Seismic excitation applied to the bottom of the numerical model

During the static analysis, the bottom boundary is fixed in the both horizontal and vertical directions and the lateral boundaries are just fixed in the horizontal direction. In dynamic problems, fixed boundary condition will cause the reflection of outward propagating waves back into the model. Therefore, during the dynamic analysis, the lateral boundary conditions are changed to the FLAC free-field boundary to eliminate wave reflections from the truncated boundaries [10].

In each dynamic analysis, 5 percent Rayleigh damping which is a typical value for geologic materials [13] is included for the soil elements in addition to the hysteretic damping already incorporated in the nonlinear stress-strain model. The damping frequency is chosen by examining the undamped behavior of the numerical model. A damped frequency of 1.8 *Hz* is used for the present model.

To avoid the numerical distortion of the propagating wave in dynamic analysis the spatial element size, Δl , must be smaller than approximately one-tenth to one-eighth of the wavelength associated with the highest frequency component of the input wave (Kuhlemeyer and Lysmer [12]):

$$\Delta L = {\lambda}/{9} \quad (7)$$

In general, the cut-off frequency for geotechnical earthquake engineering problems should be not less than 10 *Hz* [13]. Considering above criteria, element size is defined small enough to allow seismic wave propagation throughout the analysis.

3. VERIFICATION ANALYSIS

To validate the implementation of the masing rules and hysteretic damping in FLAC program via a series of FISH function, the simulation of one-zone sample with modified Byrne model is conducted by using the unit cell incorporated with the implemented rules as shown in Figure 3. The one-zone sample is modeled

with FLAC which consists of a sandy soil and a periodic motion is exerted at its base. Vertical loading is established by gravity only. Equilibrium stresses and pore pressures are installed in the soil, and pore pressure and effective stress (mean total stress minus the pore pressure) are created within the soil. The results are shown in Figures 4 and 5. Figure 4 indicates the pore pressure build-up in a single zone. It can be seen that the effective stress reaches zero after about 20 cycles of shaking (2 seconds, at 5 Hz). At this point, liquefaction can be said to occur. The stress/strain loops of the one-zone sample for several cycles are shown in Figure 5. It can be observed that shear modulus decreases with increasing shear strain. The hysteretic model seems to handle multiple nested loops in a reasonable manner. There is clearly energy dissipation and shear stiffness degradation during seismic loading.

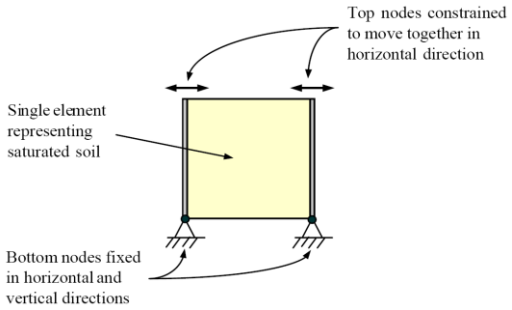

Figure 3. One-zone model in FLAC for simulating cyclic simple shear test

To evaluate the applicability of the effective stress-based analysis by FLAC, the results obtained from numerical analyses are compared with the experimental counterparts. One of the centrifuge tests related to the embankment performed in VELACS project (VErification of Liquefaction Analysis using Centrifuge Studies [6], [7]) has been chosen to evaluate the ability of the constitutive model in predicting the liquefaction phenomenon during seismic loading. It is attempted to create almost similar conditions between laboratory model test and numerical model.

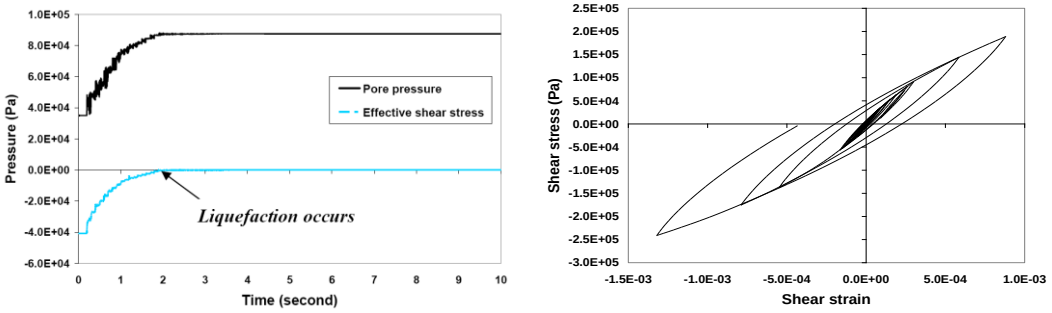

(a) (b)

Figure 4. Simulation of cyclic simple shear test of one-zone sample in FLAC: (a) pore pressure generation and effective stress time histories during the dynamic loading, and (b) hyteresis loops

The model test configuration is depicted in Figure 5(a). The numerical model constructed in FLAC is shown in Figure 5(b). The numerical results are presented and compared to those obtained from the corresponding centrifuge test. Comparisons between the computed and measured results are made in Figure 6. These comparisons show that the reference numerical model can predict the dynamic behavior of an earth dam in a reasonable manner. Due to the satisfactory modeling of the validation cases, the numerical model is then used to perform comparative study on the earth dam, as described earlier.

4. NUMERICAL RESULTS AND DISCUSSIONS

Three sets of analysis are conducted to cover all the basis of liquefaction phenomenon occurred within the earth dam and its foundation and also to evaluate the overall performance of the dam–foundation system due to the liquefaction during dynamic loading. These analyses are assigned as: Case (1): Both the dam and its foundation are susceptible to liquefaction. Case (2): Only the foundation has liquefaction potential. Case (3): Only the dam has liquefaction potential. The responses of earth dam during dynamic loading in terms of acceleration, deformation, excess pore water pressure (U_e) and excess pore water pressure ratio (R_u) are

considered. The failure mechanism of the dam can be observed in the plot of deformed grid after the dynamic loading, presented in Figure 7. It is clear that according to the simulations, the failure occurs as a progressive movement in the dam body. In Case (3), failure is observed in the both upstream and downstream slopes of dam. The overall deformation patterns of the models are the same. Horizontal displacement attained maximum values at downstream slope of the dam. The maximum horizontal and vertical displacements occur in Case (1). The shear strain increments contours are shown in Figure 8. The progressive failure is observed in slopes for all cases and failure surfaces are completely clear in the dam body. It is of interest to observe that the computational results show larger downstream lateral movements compared to the upstream side. This may be attributed to the presence of the laterally varying phreatic surface. The variable water table induced: (1) a fluid seepage force in the upstream–downstream direction and (2) a higher initial (static) shear stress distribution on the downstream side of the dam. The quantities of shear strain increments are higher for Case (1) in comparison with the other cases.

The normalized excess pore pressure ratio, (or cyclic pore pressure ratio, U_e/σ_c) is used to identify the region of liquefaction in the model. Where U_e is the excess pore pressure and σ_c is the initial effective confining stress. Note that a liquefaction state is reached when $U_e/\sigma_c = 1$. Contours of the cyclic pore pressure ratio greater than 0.99 are plotted in Figure 9. These contours show that the extent of the liquefied soils have been primarily established in the upstream region. Significant amounts of pore pressure developed after the dynamic loading can be seen in the majority of the soil material located in the upstream face and close to the dam heel. There is a larger zone of liquefaction in Case (1) rather than the other cases.

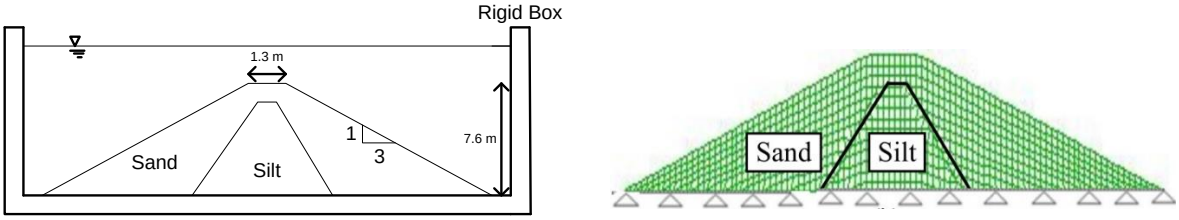

(a) (b)

Figure 5. Model configuration in rigid container: (a) centrifuge test, and (b) numerical grid constructed in FLAC

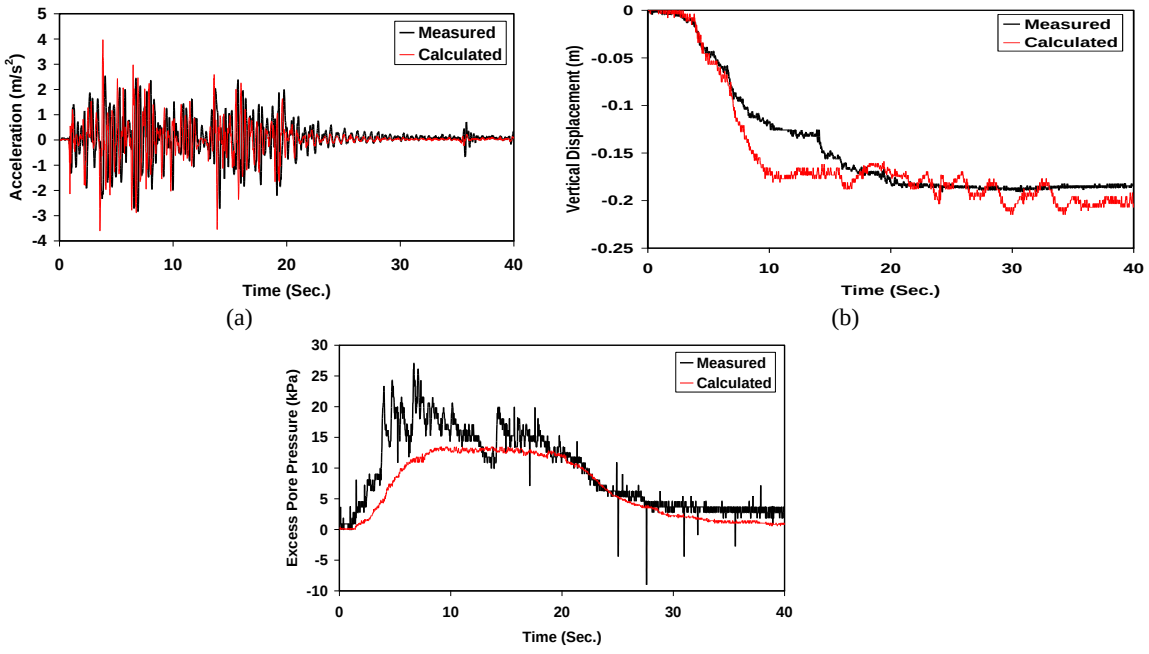

(a) (b)

(c)

Figure 6. Comparison between obtained numerical results and centrifuge test data: measured versus calculated (a) acceleration time histories, (b) displacement time histories, and (c) excess pore pressure time histories at the middle of dam height

Figure 10 (a) shows the horizontal displacement computed at the downstream slope of dam. In all cases, the horizontal displacement is seen to accumulate on a cycle-by-cycle basis. In general, lateral movements are seen to increase when the liquefaction occurs in the both dam and foundation materials. The maximum horizontal displacement (within the downstream slope) is about 1.4 *m*. The vertical displacement computed at the dam crest is shown in Figure 10(b). In general, maximum settlements take place in the crest of dam. The maximum vertical settlement at the crest is about 0.85 *m*. Figure 10(c) shows the predicted acceleration time histories at the crest of dam for all cases. It indicates that the input motion is amplified in crest for all cases. The maximum amplification occurs in Case (3) at 3.75 seconds. The computed acceleration time histories at the crest show that the input motion is amplified at the crest of dam about 1.8, 1.7 and 2 times for the Cases (1), (2) and (3), respectively.

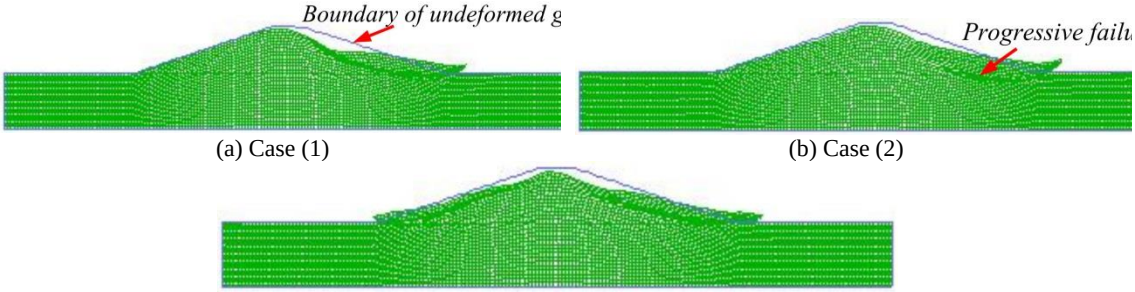

(a) Case (1) (b) Case (2)

(c) Case (3)

Figure 7. Computed deformed configuration at the end of dynamic loading (magnified by factor of 5 for clarity)

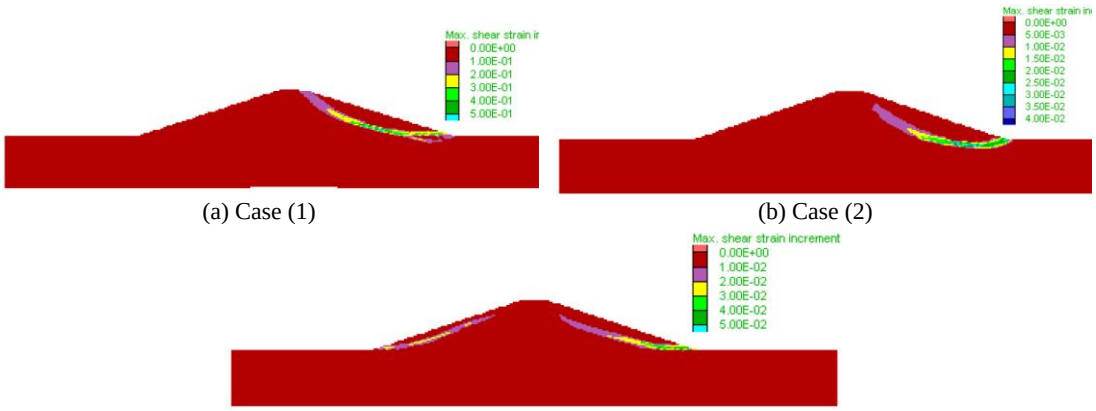

(a) Case (1) (b) Case (2)

(c) Case (3)

Figure 8. Computed shear strain increment contours at the end of dynamic loading

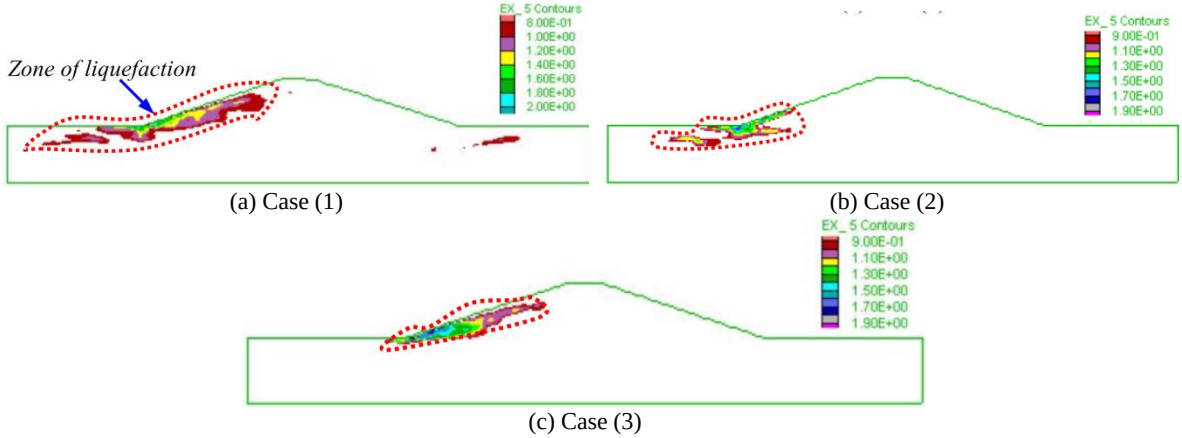

(a) Case (1) (b) Case (2)

(c) Case (3)

Figure 9. Contours of cyclic pore pressure ratio at the end of dynamic loading (values greater than 0.99)

Predicted excess pore pressures (U_e) as a function of time are shown in Figure 11(a) recorded in the zone of liquefaction at a nearby location of dam heel in foundation. It can be seen that the pore pressures increase rapidly in the time of 1 to 4 *s*, corresponding to the period of strong shaking, and then level off. However, the computed results of Case (1) are higher in the residual state comparing with the other cases. Figure 11(b) shows the evolution of the excess pore water pressure ratio (R_u) during the dynamic loading in the zone of liquefaction at a nearby location of dam heel in foundation. The excess pore water pressure ratio (R_u) increases significantly from the second 0.7 to 2.5 and then becomes constant. R_u = 1 represents a condition of 100 % pore pressure ratio and complete liquefaction.

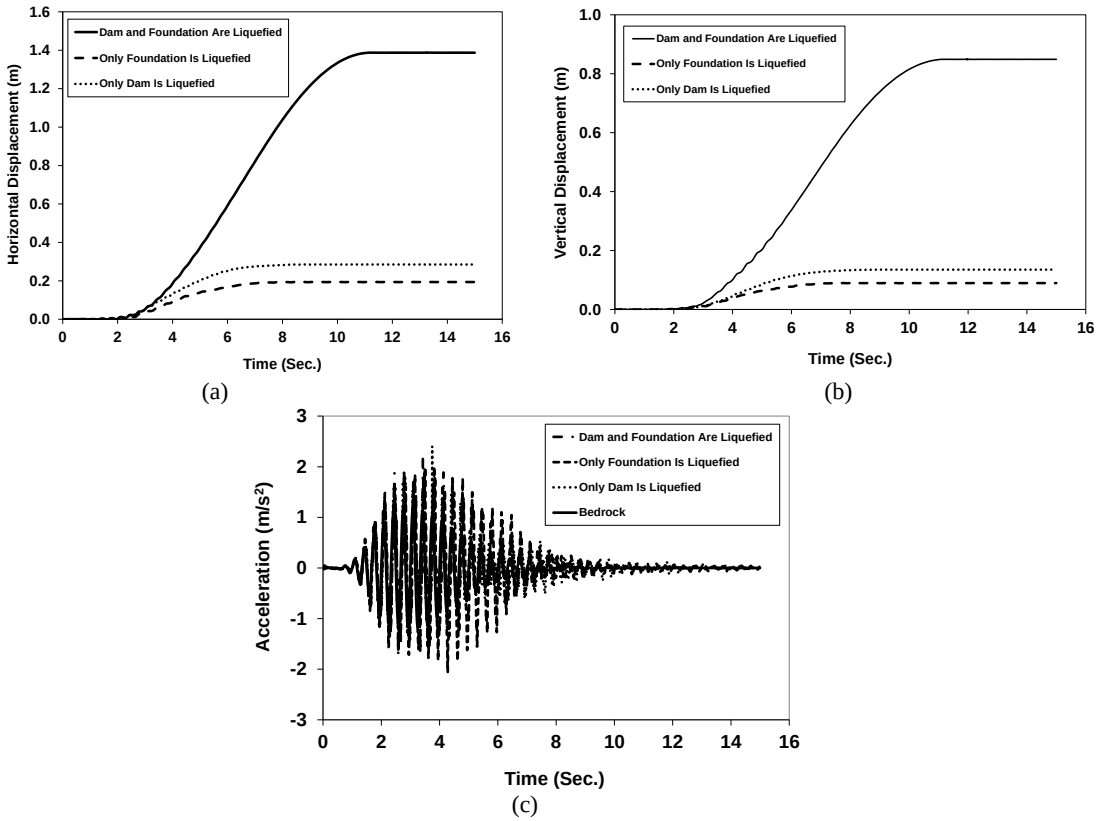

Figure 10. Computed results: (a) horizontal displacement time histories at the downstream slope of dam, (b) vertical displacement time histories, and (c) acceleration time histories at the crest of dam

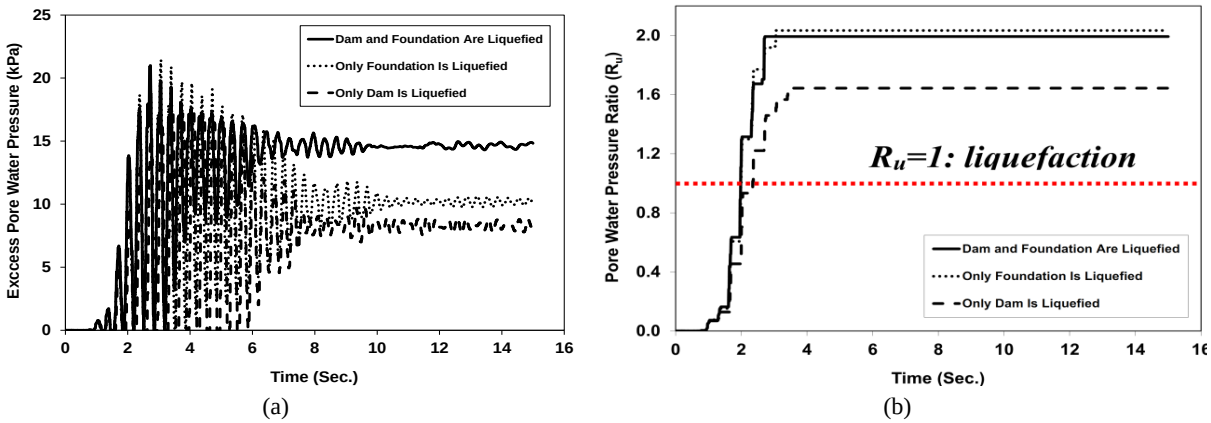

Figure 11. Computed results: (a) excess pore water pressure (U_e), and (b) excess pore water pressure ratio (R_u) time histories at the zone of liquefaction

5. CONCLUSIONS

A fully coupled nonlinear effective stress-based approach is applied to the dynamic behavior and deformation analyses of earth dam–foundation system that experiences induced liquefaction. The Finn-Byrne model with extended Masing rules is incorporated in FLAC and used for the analyses. The soil stiffness reduction and hysteretic damping changes are considered during the dynamic loading. The model's capability is demonstrated by comparing the numerical simulations with the centrifuge test results. It is observed that the numerical simulation models reasonably well the dynamic behavior of the earth dam during liquefaction phenomenon and therefore, its applicability is confirmed. It is found that, in the analyses, when liquefaction occurs in the both dam materials and foundation soils; liquefied zone at a nearby location of dam heel becomes larger and also maximum horizontal and vertical displacements occur for this case. There are larger downstream lateral movements compared to the upstream side. This may be attributed to the presence of the laterally varying phreatic surface and a higher initial (static) shear stress distribution on the downstream side of the models. The maximum amplification for acceleration occurs in the case that only the dam materials are liquefied.

6. ACKNOWLEDGMENT

The first author wants to express his sincere gratitude to the Iran's National Elites Foundation (INEF) for his moral support and encouragement.

7. REFERENCES

1. Seed, H.B. (1968), "*Landslides During Earthquakes due to Soil Liquefaction*", Journal of Geotechnical Engineering Division, American Society of Civil Engineering Vol. 94(5), pp. 1055–1123.
2. Krinitzsky, E.L. and Hynes, M.E. (2002), "*The Bhuj, India, Earthquake: Lessons Learned for Earthquake Safety of Dams on Alluvium*", Eng. Geol. (Amsterdam), Vol. 66(3–4), pp. 163–196.
3. Koga, Y. and Matsuo, O. (1990), "*Shaking Table Tests of Embankments Resting on Liquefiable Sandy Ground*", Soils and Foundations Vol. 30(4), pp. 162-174.
4. Park, Y.H., Kim, S.R., Kim, S.H. and Kim, M.M. (2000), "*Liquefaction of Embankments on Sandy Soils and the Optimum Countermeasure Against the Liquefaction*." In: Proceeding of 7th International Conference on Computer Methods and Advances in Geomechanics. Balkema, Rotterdam, Vol. 2, pp. 869-874.
5. Arulanandan, K. and Scott, R.F. (1993), "*Verification of Numerical Procedures for the Analysis of Soil Liquefaction Problems*", Conference Proceedings, Balkema, Rotterdam, Vol. 1.
6. Arulanandan, K. and Scott, R.F. (1994), "*Verification of Numerical Procedures for the Analysis of Soil Liquefaction Problems*", Conference Proceedings, Balkema, Rotterdam, Vol. 2.
7. Elgamal, A., Yang, Z. and Parra, E. (2002), "*Computational Modeling of Cyclic Mobility and Post-liquefaction Site Response*", Soil Dynamics and Earthquake Engineering. Vol. 22(4), pp. 259–271.
8. Yang, Z., Elgamal, A.H., Adalier, K. and Sharp, M.K. (2004), "*Earth Dam on Liquefiable Foundation and Remediation: Numerical Simulation of Centrifuge Experiments*", Journal of Engineering Mechanics Vol. 130(10).
9. Itasca, (2002), "*FLAC User's Guide, Version 4.0*", Itasca Consulting Group. Inc, Minnesota, USA.
10. Byrne, P. (1991), "*A Cyclic Shear-volume Coupling and Pore-pressure Model for Sand*", In Proceedings: Second International Conference on Recent Advances in Geotechnical Earthquake Engineering and Soil Dynamics (St. Louis, Missouri), Paper No. 1.24, pp. 47-55.
11. Seed, H.B. and Idriss, I.M. (1970), "*Soil Moduli and Damping Factors for Dynamic Response Analyses*", Report EERC 70-10, Earthquake Engineering Research Center. University of California, Berkeley, CA. (as cited in Kramer, 1996).
12. Kuhlemeyer, R.L. and Lysmer J. (1973), "*Finite Element Method Accuracy for Wave Propagation Problems*", Journal of Soil Mechanics and Foundations. ASCE Vol. 99, No. SM4, pp. 421-427.
13. American Society of Civil Engineers, (2000), "*ASCE 4-98 Seismic Analysis of Safety-related Nuclear Structures and Commentary*", ASCE, Virginia, USA.